Non-invasive ophthalmic imaging of adult zebrafish eye using optical coherence tomography

K. Divakar Rao*, Y. Verma, H. S. Patel and P. K. Gupta

Biomedical Applications Section, Raja Ramanna Centre for Advanced Technology, Indore 452 013, India

We describe the development of a single-mode fibre based optical coherence tomography set-up and its use for non-invasive optical imaging of adult zebrafish (*Danio rerio*) eyes. The free-space axial and lateral resolutions of the set-up were estimated to be ~ 11 and 17 μm respectively. Images of whole eye, cornea and retina acquired with the set-up have been used to estimate several ocular parameters, viz. corneal thickness, mean retinal thickness and effective refractive index of the crystalline lens.

Keywords: Eyes, non-invasive ophthalmic imaging, optical coherence tomography, zebrafish.

USE of optical techniques for biomedical imaging is a topic of considerable current interest. This is motivated by the potential of optical techniques to provide sub-millimetre resolution imaging without the need for ionizing radiation and associated risks[1]. The fundamental problem with optical imaging is that in contrast to X-rays, optical photons are strongly scattered in the tissue, which leads to blurring of the image. Several approaches can be used to pick out the useful image-bearing light from the background multiply scattered light[2]. These exploit the depolarization or loss of coherence of scattered light or the fact that scattered light emerges from the tissue in all directions and also takes a longer time to emerge compared to the unscattered (ballistic) or predominantly forward-scattered (snake-like) components. The latter essentially travels in the forward direction and so arrives earlier. Coherence gating filters-out ballistic photons with the highest image information and hence can provide images with high resolution. Optical coherence tomography (OCT), the approach that exploits coherence gating for optical imaging has emerged as a rapid, non-contact and noninvasive, high-resolution imaging technique and is finding clinical applications in ophthalmology, dermatology, etc.[3,4]. The two essential components of an OCT set-up are a low coherence light source and a Michelson interferometer set-up, one arm of which has the sample and the other arm a reference mirror. Light reflected from a layer of the sample and the reference mirror will interfere when the two path lengths are within the coherence length of the source, which is typically less than 10 μm. Axial scanning of the reference mirror helps record interferograms from different depths of the sample. Further, scanning of the reference mirror at constant speed results in Doppler shift of the reference signal. Interference of the Doppler-shifted reference signal with that reflected from a specific depth in the sample (such that the optical path length of the two interferometer arms are within coherence length) results in interference signal at Doppler frequency, which can be isolated from the rest of the backscattered signal by a suitable bandpass filter or lock-in detection system. Two-dimensional cross-sectional images and three-dimensional tomograms of the backscattered intensity distribution within the sample can be obtained by recording the interference signals from various axial and transverse positions on the sample. Two-dimensional cross-sectional images are constructed by performing measurements of the echo time delay of light at different transverse positions by scanning either the light beam or the sample.

Here we report the implementation of single-mode fibre-based OCT set-up and demonstrate its use for imaging of adult zebrafish eye (*Danio rerio*). Zebrafish, a popular aquarium fish, has emerged as a powerful new tool to understand ocular development and a variety of human diseases like retinal detachment and blindness[5–8]. The retina and lens of zebrafish eye show similar morphology as those of other vertebrates, including humans. Various mutants have been identified in zebrafish that have relevance to human disease like retinal defects. For studies in these areas, measurement of several ocular parameters of the zebrafish, like refractive index of the crystalline lens and mean retinal thickness is required. Presently, most of these measurements are being carried out on extracted eyes. We have, therefore, investigated the use of OCT for non-invasive *in situ* imaging of intact zebrafish eye. The use of OCT images to measure important ocular parameters like corneal thickness, effective refractive index of the crystalline lens and retinal thickness is discussed.

Figure 1 shows a schematic of the OCT set-up. The output of the superluminescent diode (SLD) with a centre wavelength of ~ 840 nm was coupled into a fibre optic-based Michelson interferometer using a 2×2 beam splitter designed for the wavelength used. The light beam in the

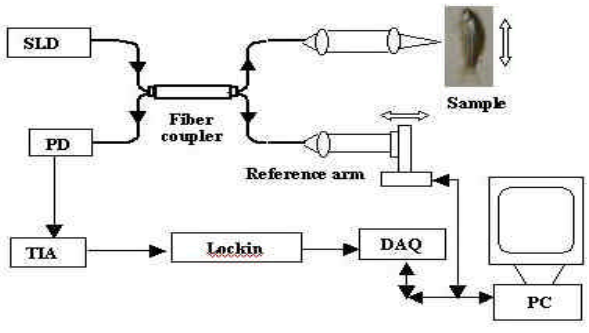

Figure 1. Schematic of experimental set-up.

*For correspondence. (e-mail: kdivakar@cat.ernet.in)

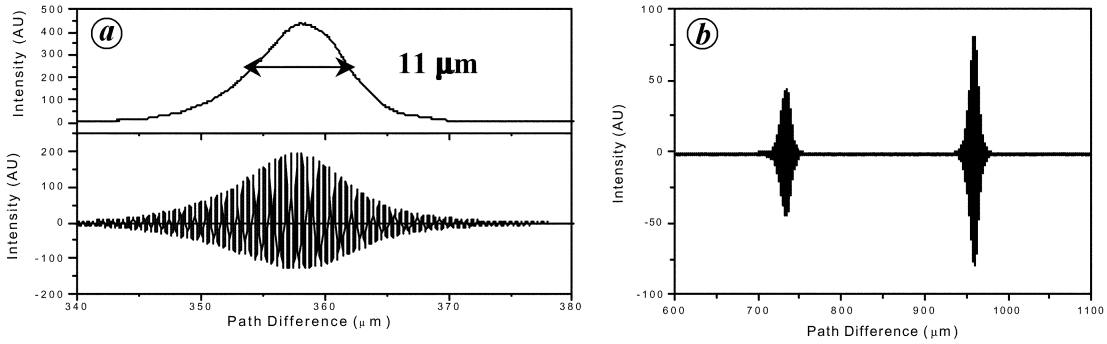

Figure 2. ***a***, Typical interferogram acquired at a Doppler frequency of ~ 22 kHz using the set-up (bottom) and its demodulated envelope. ***b***, Interferogram of a microscopic cover slip showing two peaks.

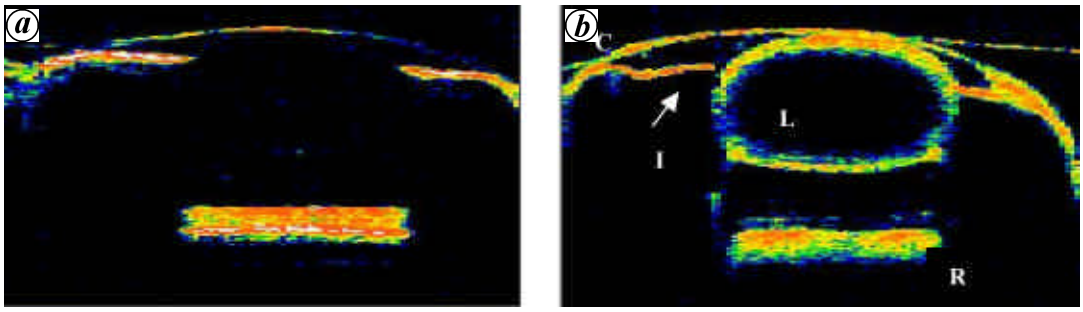

Figure 3. *In vivo* OCT image of whole eye of zebrafish under anesthesia (***a***) and ~ 30 min after dipped in 10% formalin solution. (***b***) Size of the image is 3 mm in depth and 2.0 mm in lateral direction.

sample arm was collimated and focused onto the sample with a 10X microscopic objective. The reference mirror was mounted on a linear translation stage and scanned back and forth with uniform velocity, resulting in a Doppler shift of 45 kHz. Light reflected from both the sample and reference arms was detected by a photodiode (PD) and the resulting interferogram was amplified using a transimpedence amplifier (TIA) and demodulated using a lock-in amplifier. The interferogram envelope was digitized and acquired in a PC using a data acquisition card (DAQ). Lateral scanning was done using a stepper motor. Software based on Labview was used to control the entire set-up. The free space axial and lateral resolution of the set-up were estimated to be ~ 11 and 17 μm respectively. The signal-to-noise ratio (SNR) of the set-up was measured to be ~ 100 dB. Typical image (500 × 100 pixels) acquisition time was about 1 min. The OCT images have been false-colour coded such that white represents highest backscattering intensity. The maximum power incident on the sample was ~ 0.5 mW that is well below the ANSI limits for ocular damage.

In Figure 2 *a* (bottom panel), we show a typical interferogram obtained using a mirror in the sample arm of the interferometer. The corresponding demodulated envelope is shown in the top panel. From this we estimate an axial resolution of ~ 11 μm. Figure 2 *b* shows the interferogram of a microscopic cover slip with two peaks corresponding to the air–glass and glass–air interfaces. From the measured peak separation of 231 μm (optical path length difference) and assuming glass refractive index ~ 1.5, we estimate a physical thickness of ~ 154 μm for the cover slip, which is in good agreement with the value measured using a calliper.

The lateral resolution (Δx) of the set-up is given by focal spot size on the sample, $\Delta x = (4l/p)\ (f/d)$, where f is the focal length of the imaging lens and d is the diameter of the beam on the lens. With a 10X microscopic objective, lateral resolution of 17 μm is estimated.

We used the set-up for imaging of adult zebrafish eye. The fish was procured from local aquarium suppliers. For imaging, the fish was anaesthetized using clove oil following the protocols given by Grush *et al.*[9]. Briefly, clove oil was dissolved in ethanol (1 : 10) and then mixed in 1 l of water in a glass tank, such that the clove oil concentration is about ~ 75–100 ppm. The fish lost physical movement within 10 min. When the fish showed no response to physical stimulus, it was transferred to a petri dish for imaging. After imaging, the fish was observed to revive within ~ 1 h after transfer to a freshwater tank. Due to close index matching of cornea and water during imaging, the fish eye had to be slightly projected outside the water while the gills remained in water. In Figure 3 *a* we show the *in vivo* OCT image of the whole eye of the anesthetized zebrafish kept in water. While the cornea, the anterior angle region and the retina are clearly seen, the lens is not clearly visible in the image due to close index

matching of the lens surface with the surrounding fluid. During the course of several experiments carried out to image the lens as well, it was found that the lens could be imaged with better contrast after dipping the fish in a petri dish containing 10% formalin solution for ~ 15–30 min. However the fish could not be revived in this case.

In Figure 3 *b*, we show the image after the fish was dipped in 10% formalin solution. The lens (L) as well as other ocular structures like cornea (C), iris (I), and retina (R) are clearly visible. Figure 4 shows the *in vivo* image of the cornea of zebrafish. The image is in good agreement with that published in Swamynathan *et al.*[10] using light microscopy. Corneal thickness in fish is an important parameter that is affected by environmental stress and infection. The maximum corneal thickness seen by the OCT beam was measured to be ~ 34 μm. Assuming a corneal refractive index of 1.33, the geometrical thickness of zebrafish cornea, in the region where the OCT light is perpendicular to the cornea, turned out to be 26 μm (± 11 μm). In their experiments on zebrafish cornea extracted from dissected eyeballs, Swamynathan *et al.*[10] estimated its thickness to range from 16 to 20 μm. The difference in the two measurements may be due to the difference in the protocol and may illustrate the usefulness of *in vivo* measurements. It should be noted that since the resolution of our set-up is ~ 11 μm, we could not resolve the epithelium layer of the cornea, whose thickness has been reported[10] to be ~ 8 μm. Use of a ultra-high resolution OCT set-up will be required for quantitative comparison of corneal thickness and microstructures therein.

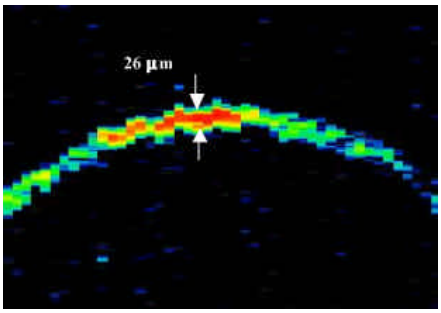

Figure 4. *In vivo* OCT image of cornea of zebrafish. Size of the image is 0.4 mm in depth and 0.9 mm in lateral direction.

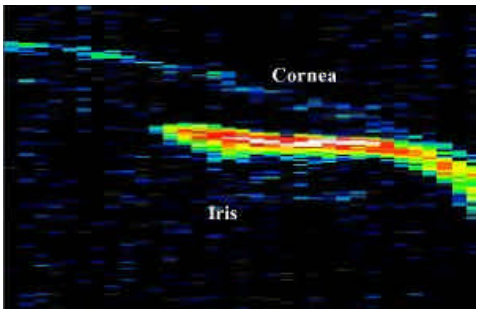

Figure 5. *In vivo* OCT image of anterior angle of the cornea with the iris of zebrafish. Size of the image is 1.3 mm in depth and 0.7 mm in lateral direction.

The anterior chamber angle is an important parameter in the structure of the eye. Narrowing of this angle increases the risk of glaucoma. Noninvasive measurement of anterior chamber angle is therefore vital for characterization of structural changes in the anterior region and changes in the intraocular pressure (IOP). *In vivo* imaging of the anterior chambers of different mutant variants of zebrafish may help in better understanding of the genetics of glaucoma. Figure 5 shows the *in vivo* OCT image of the anterior region of the eye. The anterior chamber angle of the cornea with the iris is clearly visualized.

Figure 6 shows the expanded OCT scan of the zebrafish retina with the layered structure. Due to the small retinal thickness and poor axial resolution compared to histology, assigning the layers to specific landmarks for distinct characterization is difficult. However, some broad categorization is possible. The first reflective interface posterior to the lens at the top of the image in Figure 5 represents the anterior border of the retina (vitreo–retinal interface) with the retinal nerve fibre layer (RNFL) at the vitreous interface. The outermost band is thought to be that of the retinal pigment epithelium (RPE)–choriocapillaris complex showing high scattering. Assuming a retinal refractive index of 1.38 and considering the band above RPE, the retinal thickness has been estimated as 123 ± 12 μm. This is quite reasonable in comparison with the mean retinal thickness of ~ 85 μm for wild-type zebrafish reported by Link *et al.*[11] considering the fact that their measurements are on resected eyes.

In Figure 7 we show the OCT image of the whole eye of a zebrafish when dipped in 10% formalin solution, taken at a different lateral position. Along the apex of the lens (when the OCT beam was exactly perpendicular to the cornea) some scattering inside the lens was also seen, indicating that the crystalline lens is of a gradient index type. An interesting observation was that although the lens of the fish eye is known to be spherical in shape, the diameters of the lens as measured by OCT were different along the axial and lateral directions. This is because, while in axial direction the measured diameter is the optical length

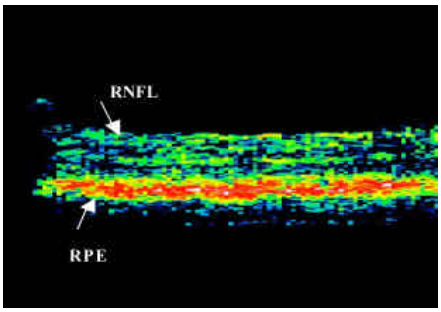

Figure 6. *In vivo* OCT image of retina of zebrafish. Size of the image is 1 mm in depth and 0.7 mm in lateral direction.

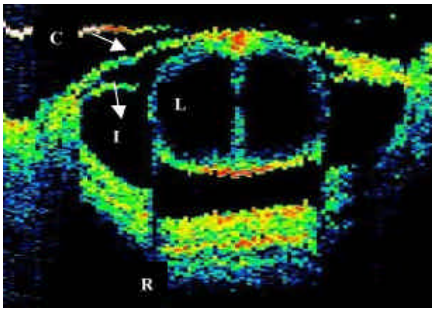

Figure 7. OCT image of whole eye of zebrafish. Size of the image is 3 mm in axial and 2.2 mm in lateral direction.

of the lens (geometrical path × effective refractive index), in the lateral direction it is the true geometrical diameter. The difference in the ratio of the measured diameters can be used to estimate the effective index of refraction of the lens medium. From the image shown in Figure 2, effective refractive index of ~ 1.43 was estimated for the zebrafish crystalline lens at the centre wavelength of the source (840 nm). The crystalline lens of the fish is usually assumed to be spherical with a gradient refractive index that varies from approximately 1.35–1.38 at the surface to 1.55–1.57 at the core of the lens[12,13].

The refractive index of the fish lens was also measured using focus-tracking method described by Wang *et al.*[14]. The sample arm light was focused using a high numerical aperture (NA) microscopic objective (20X) with the focal plane set initially at the top surface of the lens. This was achieved by monitoring the intensity of the A-scan peak, and maximizing the corresponding peak of the lens surface. Once the focus was set at the top of the lens surface, the objective was moved a distance Δx such that the bottom surface of the lens came in focus. The corresponding change in the reference mirror position (Δy) required to get back the A-scan peak intensity was noted. The effective refractive index was determined using the expression[14]

$$n^2 = \frac{1}{2}\left[NA^2 + \sqrt{NA^4 + 4(n_0^2 - NA^2)\left(\frac{\Delta y}{\Delta x}\right)^2} \right], \quad (1)$$

where n_0 is the refractive index of the surrounding medium of the tissue. Before applying this technique to fish lens, we used it to measure the refractive index of quartz window. The measured value of 1.445 @840 nm was found to be in good agreement with the reported value[14]. From the measurements, we estimate the effective (integrated) refractive index of the fish lens as ~ 1.43 @840 nm within 3% rms deviation.

The effective refractive index can also be computed assuming the refractive index variation along the beam direction to be of parabolic form[15] given by

$$n(z) = n_0\sqrt{1 - z^2/a^2}, \quad (2)$$

where n_0 is the maximum refractive index at the centre of the lens and a is a constant that indicates the steepness of the gradient in the refractive index. The effective refractive index of the lens (n_{eff}) as seen by the OCT beam is then given by

$$n_{\text{eff}} = \frac{\int_{-r}^{+r} n(z)\mathrm{d}z}{2r}, \quad (3)$$

where $\int_{-r}^{+r} n(z)\mathrm{d}z$ is the total optical path along the apex of the lens as seen by the OCT beam and r is the radius of the spherical lens. Using OCT, r was measured to be 0.46 mm. The index of the lens surface is reported to be in the range 1.35–1.38 at 632.8 nm[12,13]. As the OCT reflection (@840 nm) from the lens surface was feeble (possibly due to close index matching of lens with surrounding fluid), we assume the index at the lens surface to be 1.34. We calculated the effective refractive index from eq. (3) using different values of core index n_0 in the range 1.54–1.59. Using $n_0 = 1.54$ yields effective refractive index $n_{\text{eff}} \sim 1.476$, closer to the experimentally measured value.

The relative error in the estimation of effective refractive index of the crystalline lens using the OCT method can be estimated by

$$\frac{d n_{\text{eff}}}{n_{\text{eff}}} = \frac{d D_z}{D_z} - \frac{d D_x}{D_x}, \quad (4)$$

where D_z is the diameter of the lens along the axial direction, D_x is the diameter of the lens along the lateral direction, and dD_z and dD_x are the uncertainties in measurement of the diameters along the axial and lateral directions respectively. Using the values $dD_z \sim 11$ μm (axial resolution), and $dD_x \sim 27$ μm (lateral resolution with 5X objective), the relative error $|d n_{\text{eff}} / n_{\text{eff}}|$ is estimated to be ~ 2%. Taking the measured value of $n_{\text{eff}} \sim 1.43$, the absolute error in the effective refractive index estimate is $dn_{\text{eff}} \sim 0.029$. The discrepancy between the estimated effective refractive index (1.43) and computed value (1.476) is therefore not appreciable. Further, to the best of our knowledge there are no experimental measurements of refractive index of zebrafish lens. Even though the fish could not be revived after these measurements, it did not require separation of the lens from the fish eye unlike the previous studies by Garner *et al.*[12], who used MRI for determination of gradient index of fish lens after physical separation. The OCT method allows the fish to be intact for further biological/biochemical studies, if necessary.

In summary, single-mode fibre-based OCT set-up has been developed and ophthalmic imaging of adult zebrafish eyes has been carried out. The measured corneal and retinal thicknesses are in reasonable agreement with the previously reported values. The effective refractive index n_{eff} was estimated to be ~ 1.43 (± 0.03) and was independ-

ently confirmed with the index measured using focus tracking method.

1. Ramachandran, H., Imaging through turbid media. *Curr. Sci.*, 1999, **76**, 1334.
2. Dunsby, C. and French, P. M. W., Techniques for depth-resolved imaging through turbid media including coherence-gated imaging. *J. Phys. D*, 2003, **36**, R207.
3. Fujimoto, J. G., Optical coherence tomography for ultrahigh resolution *in vivo* imaging. *Nature Biotechnol.*, 2003, **21**, 1361.
4. Bouma, B. E. and Tearney, G. J. (eds), *Handbook of Optical Coherence Tomography*, Dekker, New York, 2002.
5. Barot, B. A. and Zon, L. I., Realizing the potential of zebrafish as a model for human disease. *Physiol. Genomics*, 2000, **2**, 49–51.
6. McMahon, C., Semina, E. V. and Link, B. A., Using zebrafish to study the complex genetics of glaucoma. *Comp. Biochem. Physiol. Part C: Toxicol. Pharmacol.*, 2004, **138**, 343–350.
7. Goldsmith, P. and Harris, W. A., The zebrafish as a tool for understanding the biology of visual disorders. *Semin. Cell Dev. Biol.*, 2003, **14**, 11–18.
8. Glass, A. S. and Dham, R., The zebrafish as model organism for eye development. *Ophthalmic Res.*, 2004, **36**, 4–24.
9. Grush, J., Noakes, D. L. G. and Moccia, R. D., The efficacy of clove oil as an anesthetic for the zebrafish, *Danio rerio* (Hamilton). *Zebrafish*, 2004, **1**, 46–53.
10. Swamynathan, S. K., Crawford, M. A., Robinson Jr., W. G., Kanungo, J. and Piatigorsky, J., Adaptive differences in the structure and macromolecular compositions of the air and water corneas of the 'four-eyed' fish (*Anableps anableps*). *FASEB J.*, 2003, **17**, 1996–2005.
11. Link, B. A., Gray, M. P., Smith, R. S. and John, S. W. M., Intraocular pressure in zebrafish: comparison of inbred strains and identification of a reduced melanin mutant with raised IOP. *Invest. Ophthalmol. Vis. Sci.*, 2004, **45**, 4415–4422.
12. Garner, L. F., Smith, G., Yao, S. and Augusteyn, R. C., Gradient refractive index of the crystalline lens of the Black Oreo Dory (*Allocyttus niger*): comparison of magnetic resonance imaging (MRI) and laser ray-trace methods. *Vision Res.*, 2001, **41**, 973–979.
13. Acosta, E., Vazquez, D., Garner, L. and Smith, G., Tomographic method for measurement of the gradient refractive index of the crystalline lens. I. The spherical fish lens. *JOSA A*, 2005, **22**, 424–433.
14. Wang, X., Zhang, C., Zhang, L., Xue, L. and Tian, J., Simultaneous refractive index and thickness measurements of bio tissue by optical coherence tomography. *J. Biomed. Opt.*, 2002, **7**, 628–632.
15. Rowe, M. P., Engheta, N., Easter, Jr. S. S. and Pugh, Jr. E. N., Graded-index model of a fish double cone exhibits differential polarization sensitivity. *JOSA A*, 1994, **11**, 55–70.

ACKNOWLEDGEMENTS. We thank M. R. Jathar for help with triggered data acquistion and synchronization of the set-up and M. Sharma for useful suggestions regarding anesthesia.

Received 20 October 2005; accepted 7 February 2006